Grain alignment and polarization in molecular cloud

SOFIA Tele-talk, Dec. 16, 2020

Le Ngoc **Tram** - SOFIA Postdoc Fellow

Universities Space Research Association, Nasa Ames Research Center, CA, USA

on perhaps of

Collaborations

- Thiem Hoang (KASI, Korea)
- Hyeseung Lee (KASI, Korea)
- William T. Reach (USRA-SOFIA, USA)
- Archana Soam (USRA-SOFIA, USA)
- Simon Coudé (USRA-SOFIA, USA)
- Enrique Lopez-Rodriguez (USRA-SOFIA, USA)
- David Chuss (Villanova, USA)
- Joseph Michail (Northwestern University, USA)
- Fabio Santos (MPIfA, Heidelberg, Germany)
- Antoine Gusdorf (LPENS, ENS, France)
- Pierre Lesaffre (LPENS, ENS, France)
- Pham Ngoc Diep (VNSC, Vietnam)
- Nguyen Bich Ngoc (GUST, Vietnam)

SOFIA Stratospheric Observatory for Infrared Astronomy USRA NASA

Contents

1. Introductions and motivations

- Magnetic field (B-field) is believed to play a substantial role in the star-formation processes (Crutcher 2012)
- Direct measurement of B-field is a difficult issue
  → Indirect methods:
    - the dust polarization (SOFIA/HAWC+ and others)
    - the Zeeman effect
    - the Goldreich-Kylafis effect
    - the Faraday effect
    - the synchrotron emission

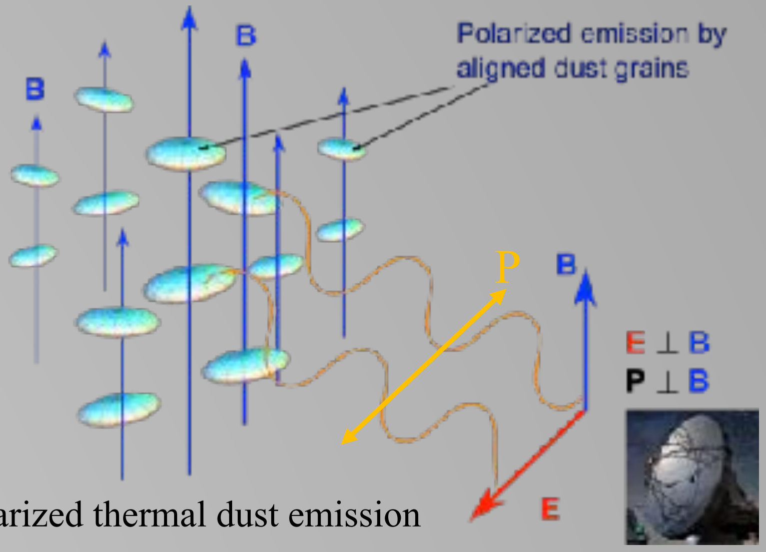

Polarized thermal dust emission

- Radiative torque (RAT) alignment theory is a popular theory describing grain alignment and polarization (Lazarian & Hoang 2007; Andersson et al. 2015)
  → implemented to POLARIS code (Reissl & Bauer)
- One of the key predictions of the RAT theory: the polarization degree correlates with the intensity of the radiation field (or equivalently dust temperature, see e.g., Lee et al. 2020)
- Observational Question: p increases and then decreases as T_d increases?

(RAT prediction) (Opposite to RAT prediction)

Planck collaboration 2018

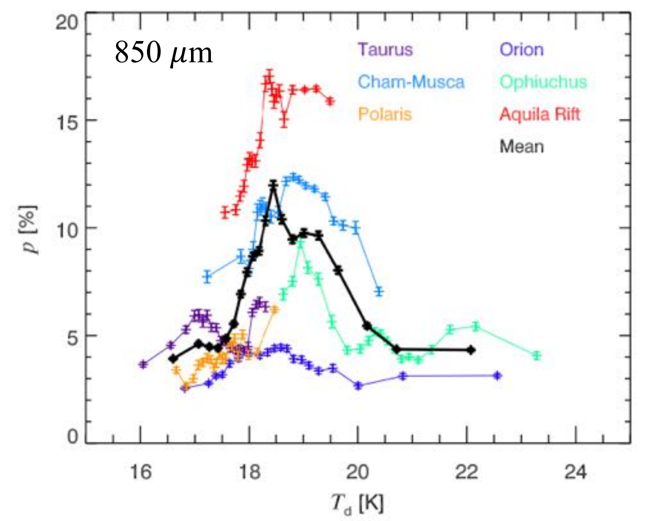

1. Introductions and motivations

Planck collaboration 2018

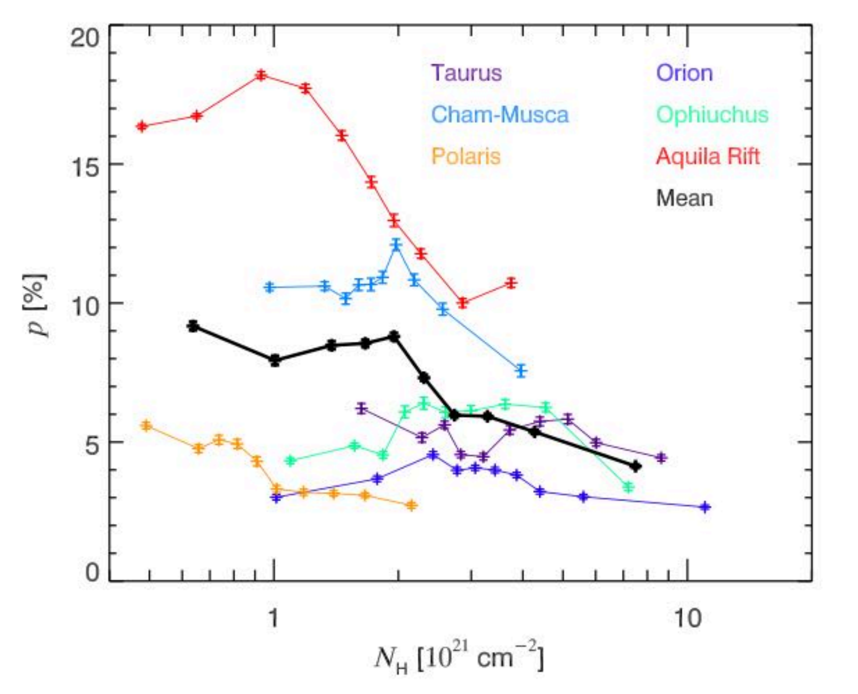

❖ Observations report the anti-correlation of p(%) to N_H

→ Loss of grain alignment toward dense medium (Whittet et al. 2008)

→ Turbulent structure of magnetic field within the scale of the beam size (e.g., Jones & Whittet 2015; Planck Collaboration et al. 2015).

1. Introductions and motivations

Oph-A observations

Santos et al. 2019; Tram, Hoang et al. 2020b

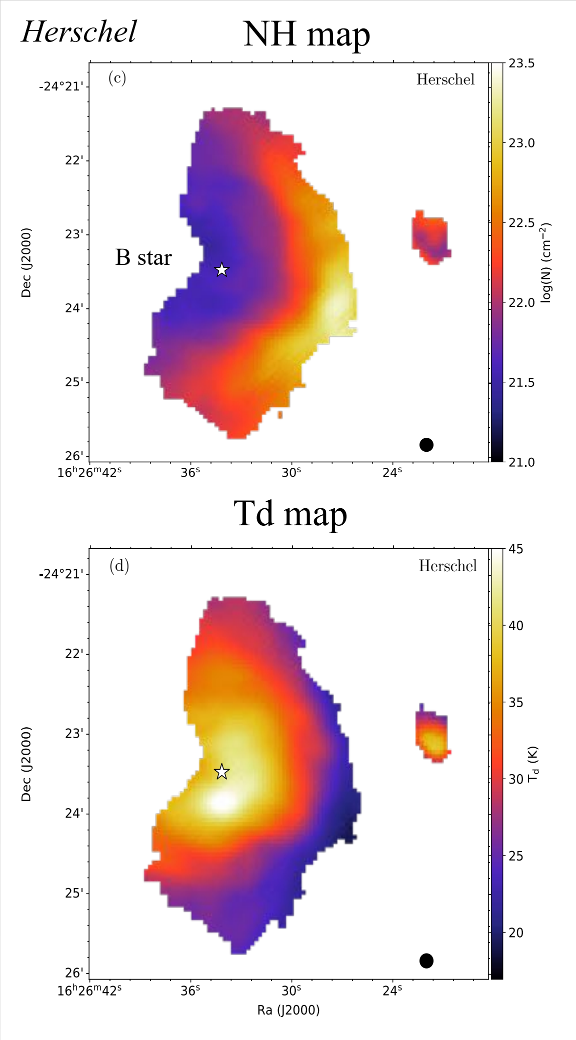

SOFIA/HAWC+ (Tram, Hoang et al. 2020b)

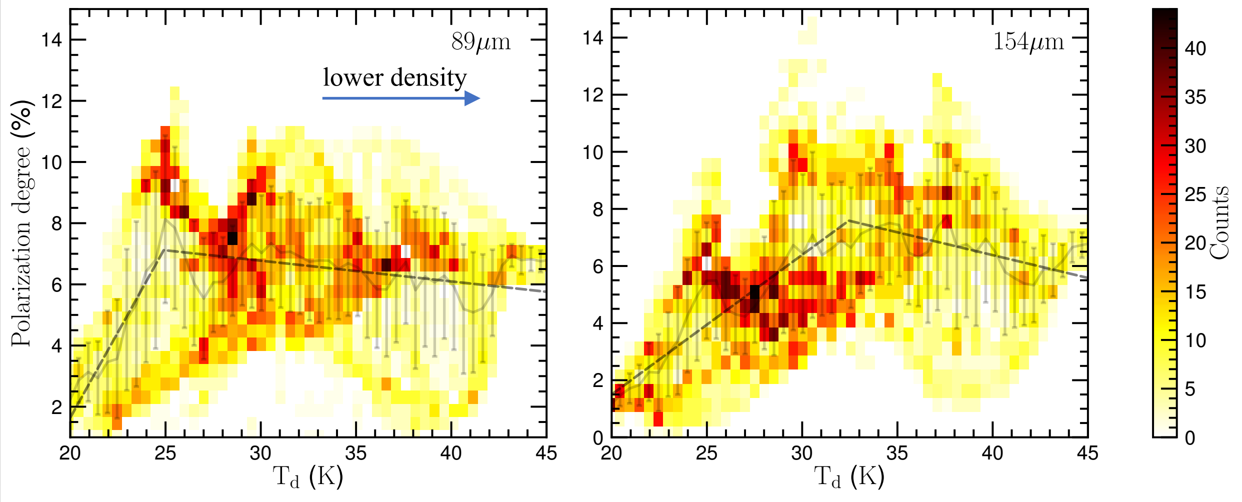

2D histogram of the dust polarization degree and dust temperature for 89 μm (left panel) and 154 μm (right panel). The gray lines show the binning weighted-mean of the data and the error bars represent the standard deviation within the bin. The black dashed lines show the best t of the piecewise linear function to the data.

SOFIA/HAWC+ (Santos et al. 2019)

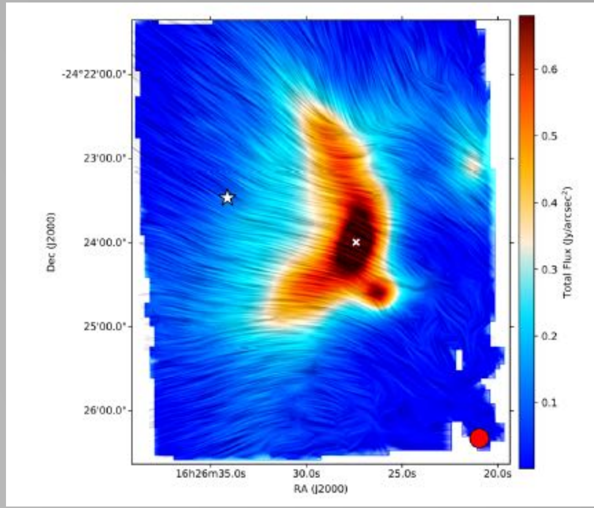

LIC maps of the inferred magnetic field

- *p* increases and decreases with Td
- *p* decreases toward + **lower gas density**
  + **higher dust temperature**

  → ~~Loss of grain alignment toward dense medium~~

- B-field is "well ordered" in Oph-A
  → Turbulent of B-field within the scale of the beam size ???

2. Radiative torque disruption (RATD) mechanism (Hoang, Tram et al. 2019)

❖ Large grains exposed in a strong radiation field (or high dust temperature in equivalent) can be spin-up very fast by RAT.

$$\omega_{\rm RAT} = 7.6\times10^{10}\gamma a_{-5}^{1.7}\bar{\lambda}_{0.5}^{-1.7}U_6^{1/3} \text{ rad s}^{-1}$$

Note: rotating grain is damped by (Lee et al. 2020)

- gas collision $\tau_{\rm gas} \sim a n_{\rm H}^{-1} T_{\rm gas}^{-1}$
- IR re-emission $\tau_{\rm em} \sim \frac{a^3}{Q_{\rm abs}} U^{-1} T_{\rm d}^2$

❖ The induced centrifugal stress $S = \rho\omega^2 a^2/4 \Rightarrow \omega_{\rm crit} = \frac{2}{a}\left(\frac{S_{\rm max}}{\rho}\right)^{1/2}$ rad s^{-1}

❖ For sufficiently high rotation rate, the induced centrifugal force can exceed the binding force ($S_{\rm max}$) that holds the grain's structure
→ disrupts the large grain into smaller species.

- $S_{\rm max} = 10^6$-10^8 erg cm^{-3}: composite structure (Hoang 2019)
- $S_{\rm max} = 10^9$-10^{10} erg cm^{-3}: compact structure (Draine & Salpeter 1979; Burke & Silk 1974)
- $S_{\rm max} = 10^{11}$ erg cm^{-3}: ideal materials (i.e., diamond, Hoang et al. 2019)

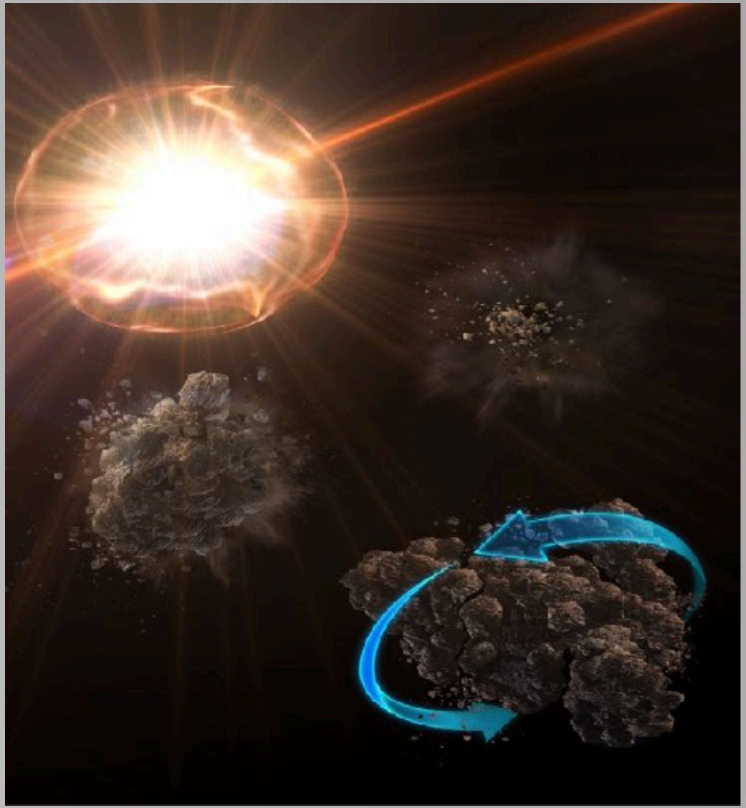

Hoang, Tram et al. 2019 Nature Astronomy

2. Dust Polarization (Dustpol) model (Lee et al. 2020)

❖ DUSTPOL models

- the starlight polarization and polarized thermal dust emission
- simultaneously consider RAT + RATD

$U = u_{\rm rad}/u_{\rm ISRF}$ radiation strength (dimensionless)

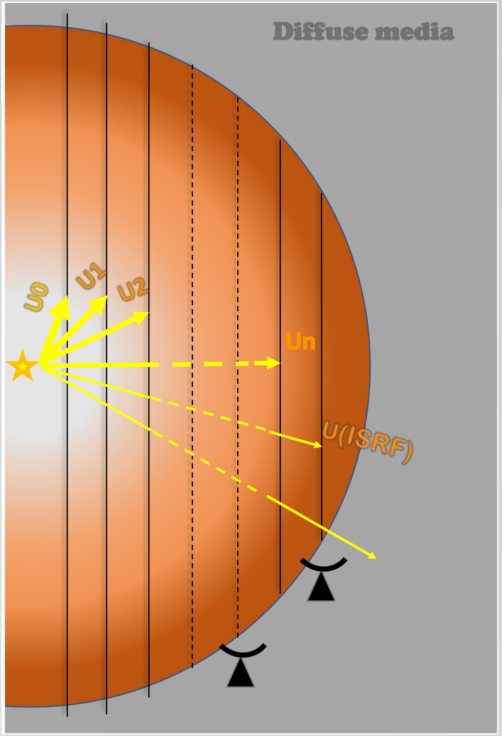

RAT

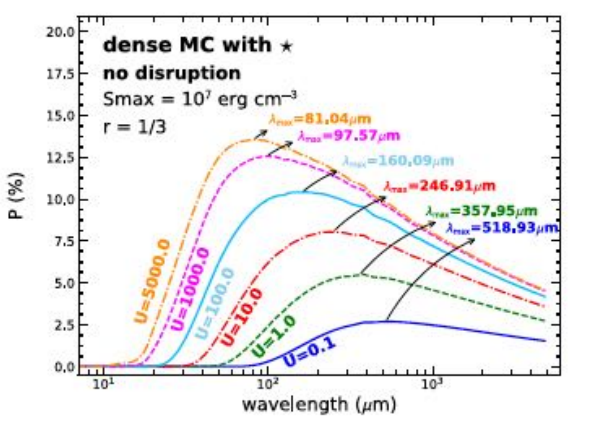

RAT+ RATD

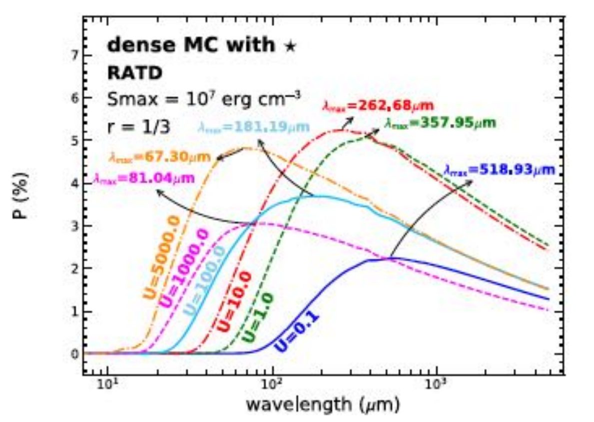

$n_{\rm H}$=const.

Dustpol model

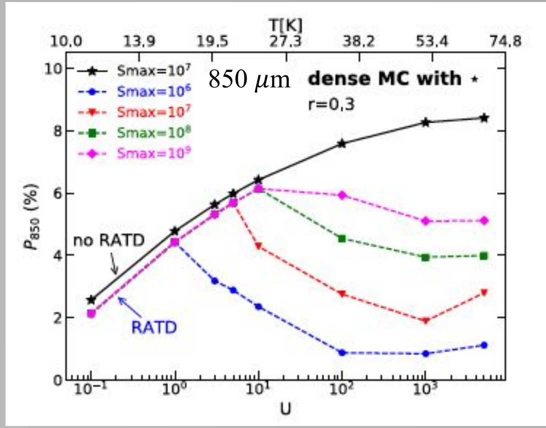

Planck observations

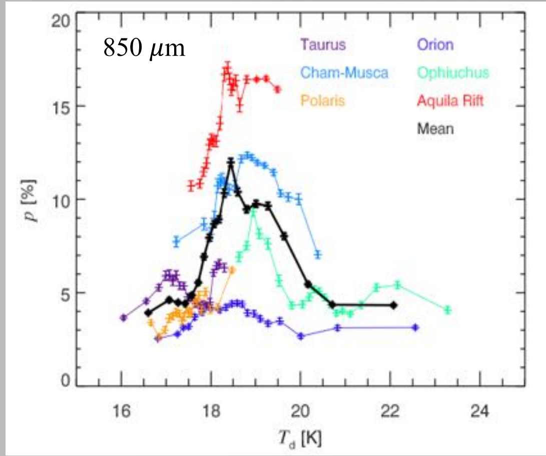

❖ Without RATD: monotonic increase of $p(\%)$ with $T_{\rm d}$ (classical RAT)

❖ With RATD:

- $p(\%)$ first increases: disruption does not occur → classical RAT
- $p(\%)$ then decreases: disruption occurs

$T_{\rm d,threshold}$ depends on the $(U, S_{\rm max}, n_{\rm H})$

2.1 Applications to Oph-A (Tram, Hoang et al. 2020b)

Numerical setup

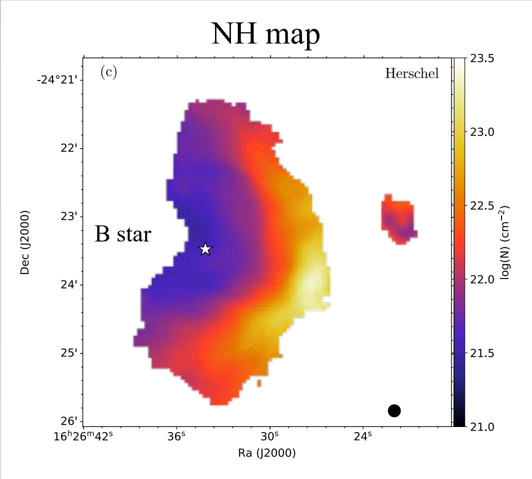

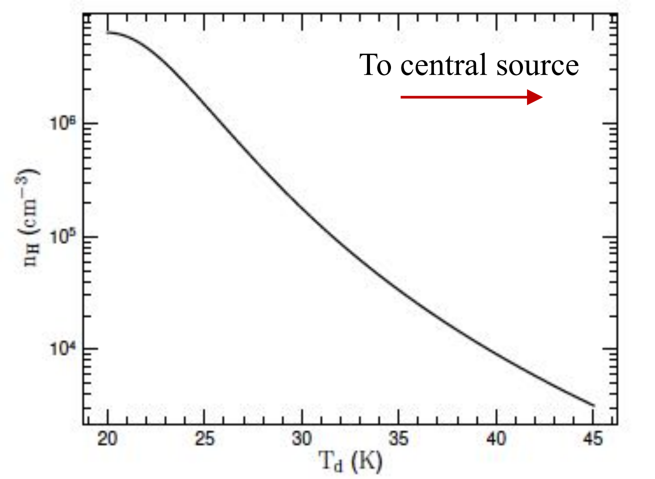

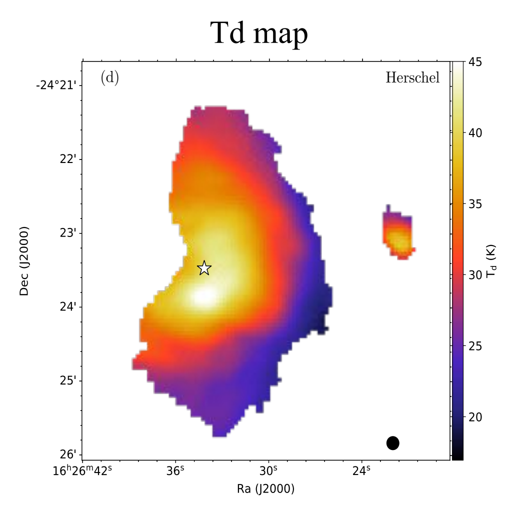

- n_H-T_d from spherical model (Santos et al. 2019)
- T_d from observations
- Grain-size distribution (β)
- $T_{gas} \sim 20$ K
- $\bar{\lambda} = 0.3\ \mu m$ ($T_* = 1.5\times10^4$K)

Numerical results

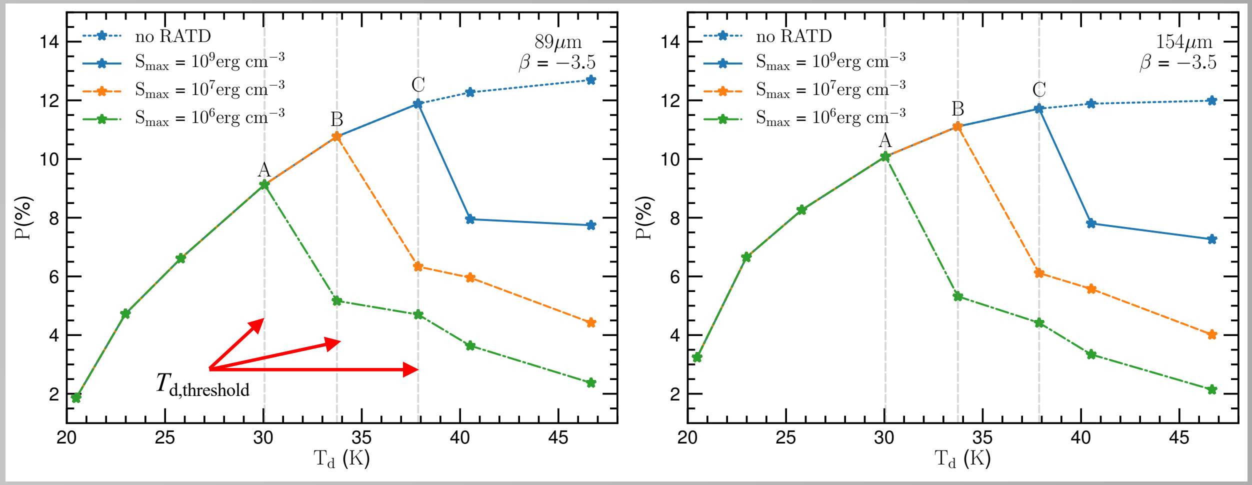

- $T_d < T_{d,threshold}$: weak radiation (low-T_d) and dense gas (high N_H) → damping is substantial → no RATD → p(%) increases as T_d increases
- $T_d > T_{d,threshold}$: strong radiation (high-T_d) and less dense gas (low N_H) → damping is inefficient → RATD → p(%) decreases as T_d increases
- More compact grains, harder to be disrupted

2.1 Applications to Oph-A (Tram, Hoang et al. 2020b)

Interpret SOFIA/HAWC+ observations

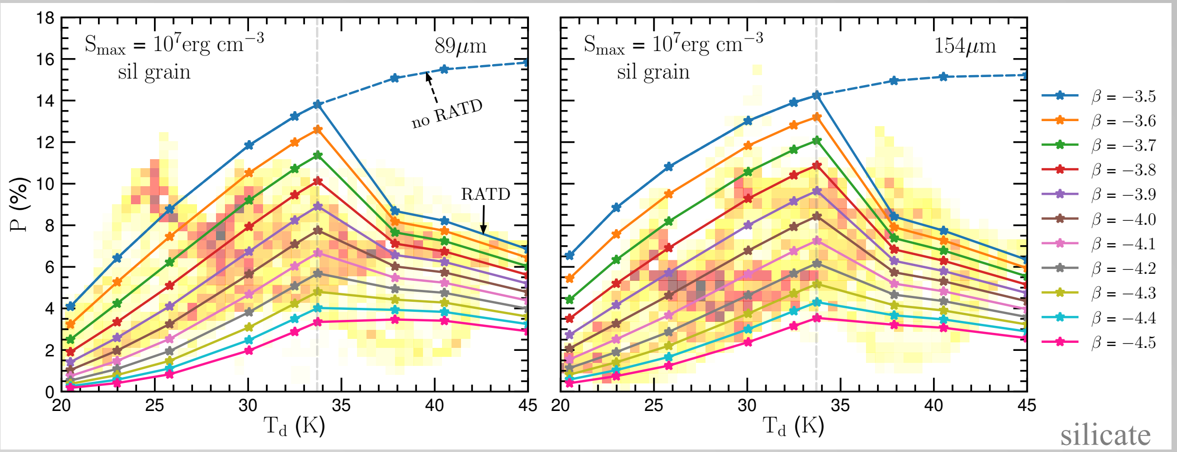

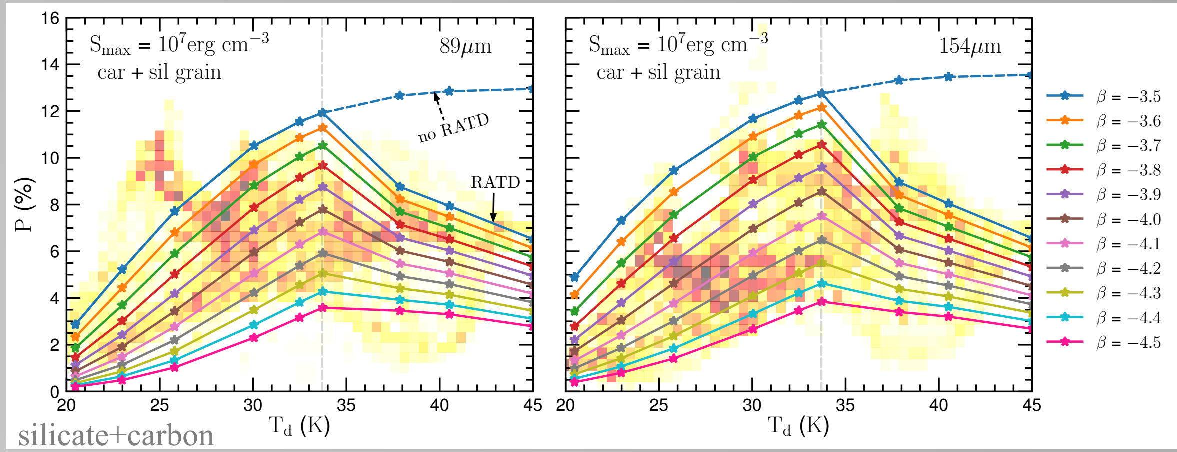

Table 1. χ^2 of the models with a single aligned silicate grains (Figure 11) and a combination of aligned carbonaceous and silicate grains (Figure 12) to observations computed by

$$\chi^2 = \frac{1}{N}\sum_i^N (P^i_{\rm obs} - P_{\rm mod})^2/P^i_{\rm obs}$$

with N the number of data points

	χ^2(89 μm, f_{max} = 1)		χ^2(154 μm, f_{max} = 0.35)	
β	sil grain	car+sil grain	sil grain	car+sil grain
-3.5	4.99	3.41	10.62	7.40
-3.6	3.45	2.65	7.60	5.69
-3.7	2.36	2.03	5.12	4.15
-3.8	1.68	1.59	3.25	2.86
-3.9	1.37	1.35	1.98	1.89
-4.0	1.34	1.31	1.26	1.28
-4.1	1.53	1.44	1.01	1.02
-4.2	1.86	1.71	1.09	1.04
-4.3	2.26	2.08	1.41	1.28
-4.4	2.71	2.50	1.84	1.67
-4.5	3.15	2.94	2.33	2.12

- Assuming that all dust grains follow a power-law size distribution.
- Our modeling results could successfully reproduce both the rising and declining trends of the observational data.
- We show that the alignment of only silicate grains or a mixture of silicate-carbon grains within a composite structure can reproduce the observational trends
- Grains in Oph-A cloud have a composite structure
- The grain-size distribution has steeper slope $\beta < -3.5$ (ISM).

2.1 Applications to 30 Dor (Tram et al in prep)

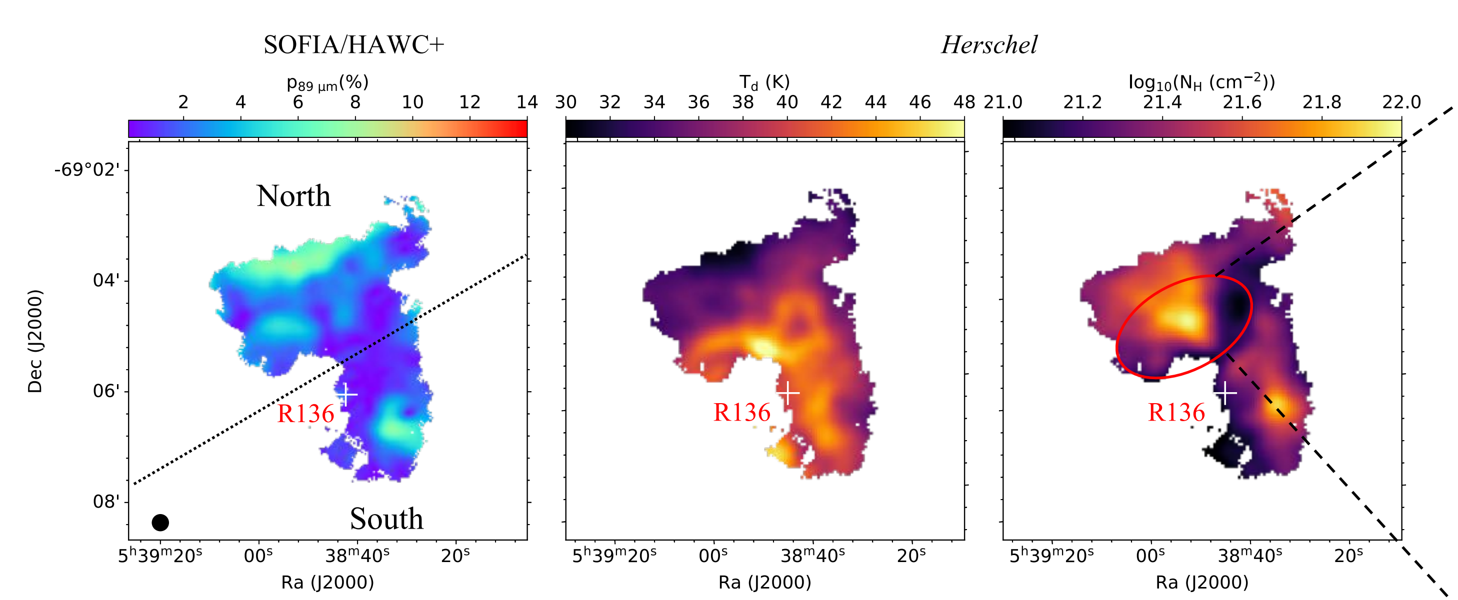

Toward R136 → ← Toward R136

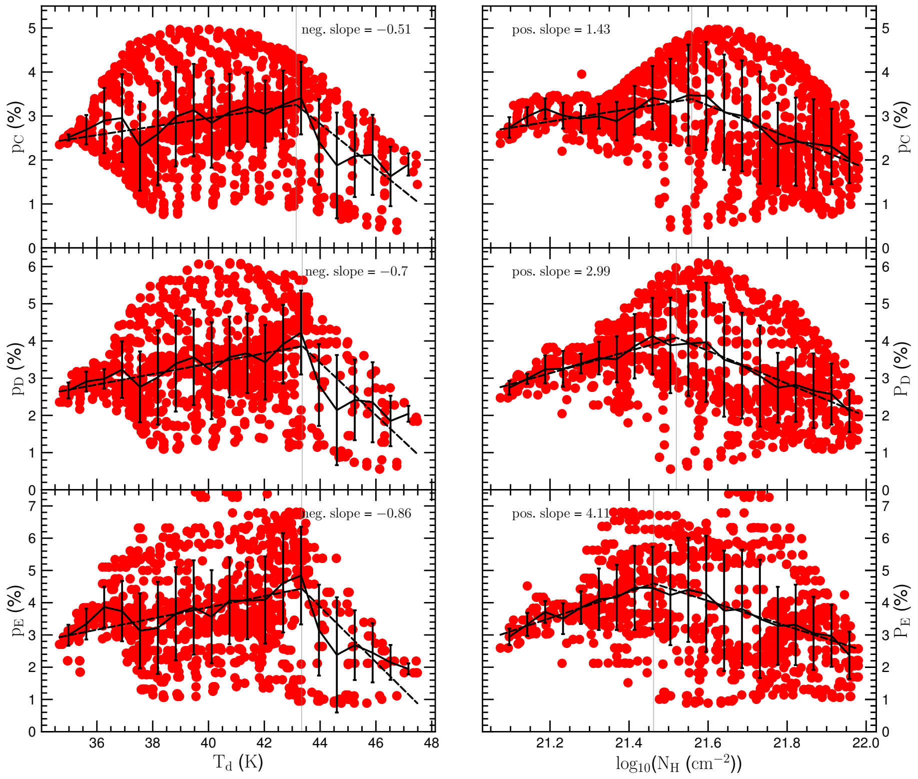

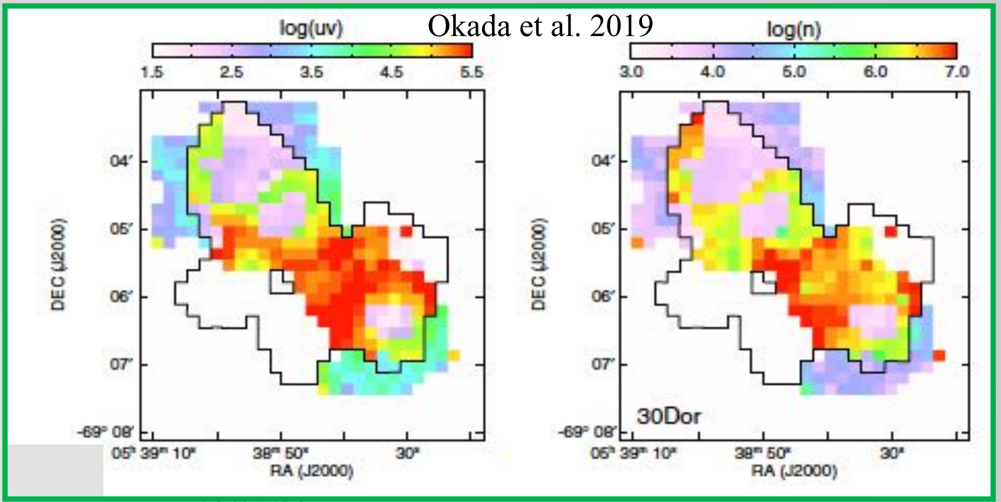

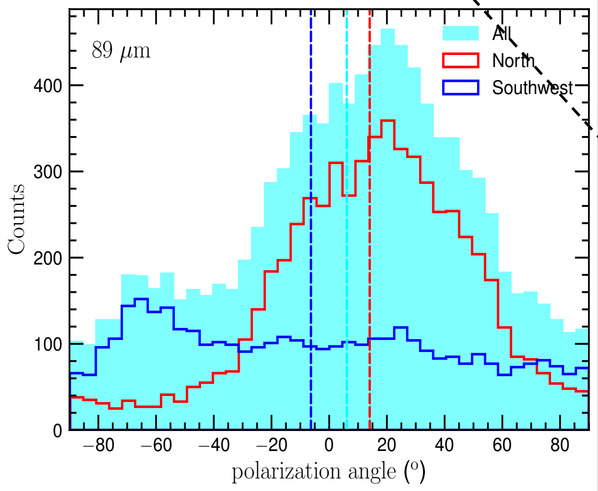

- There are 2 mains regions in 30 Dor: North, South
- Dust grains are heated more efficiently close to the radiation source
- Gas is denser farther away from the source
  → Like Oph-A

2.2 Limitations and perspectives of DUSTPOL code

- DUSTPOL's input parameters are the local n_H and the local T_d
  - first controls the damping process of the rotating grains,
    - its value is derived from a spherical model
  - second denes the angular rotational rate of grains.
    - its value is adopted from observations (projection effect -- the actual value could be higher than these)
- B-field is assumed to be uniform
  - In realistic, the variation of B-field along the l.o.s could reduce p(%) but not change the p(%)-T_d trend.

- DUSTPOL's input parameters are the local parameters.
  - prescription will be easy to incorporate into more elaborate models that have better physical treatments for the gas and dust properties
    - 3D radiative dust modeling codes (e.g., Dullemond et al. 2012; Liseau et al. 2015)
- Variation of B-field is being updated into the new version of DUSTPOL code

3. Polarization hole

Starless cores (Jones et al. 2015)

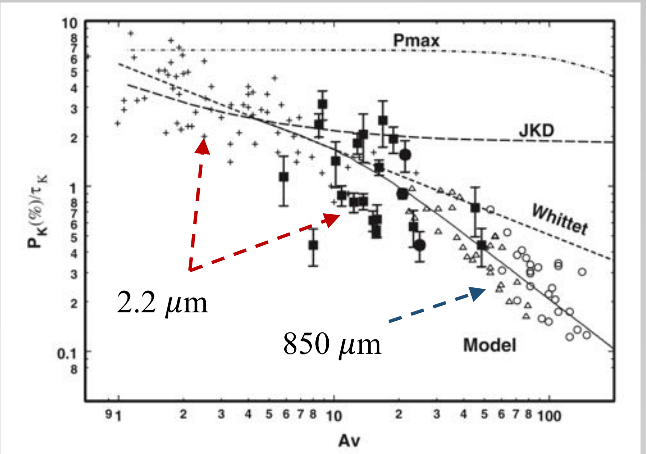

Protostellar cores (Hull et al. 2014)

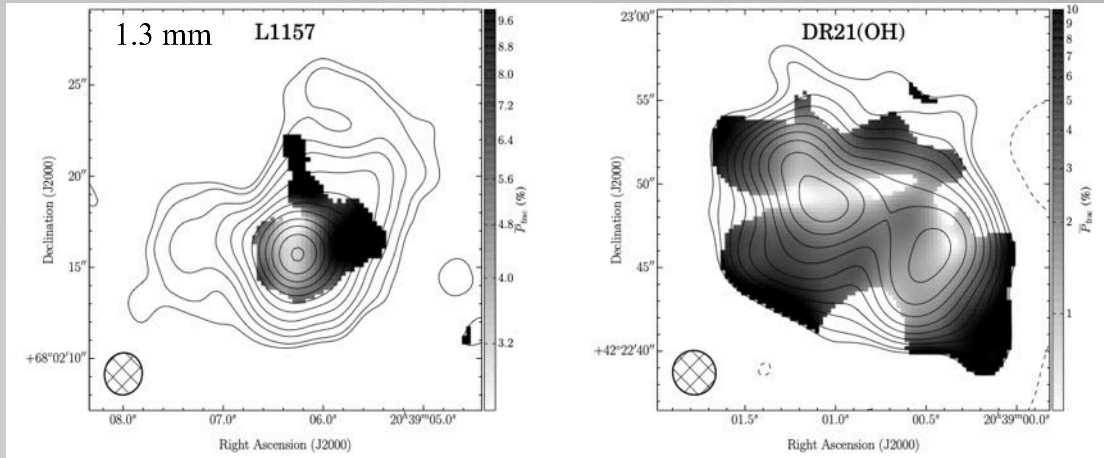

Contour: dust continuum
Grayscale: $p(\%)$

Lee et al. 2020

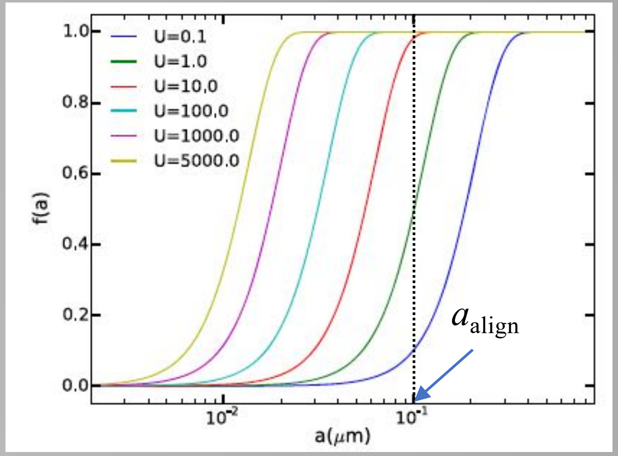

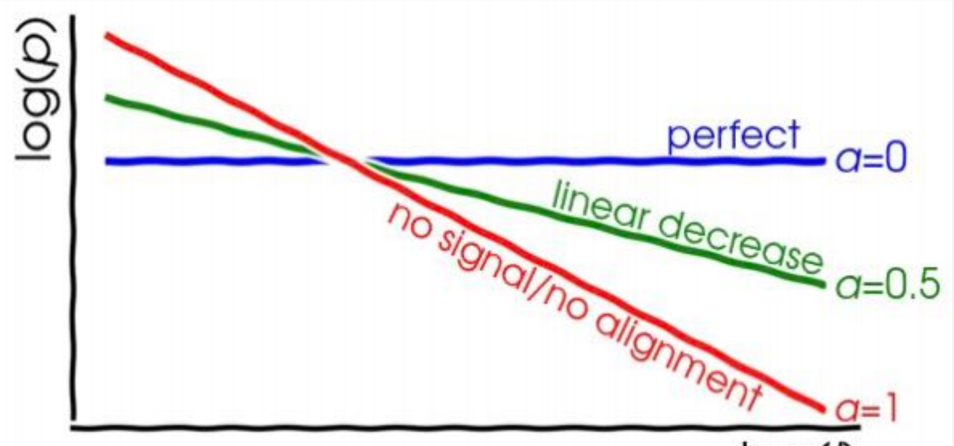

Pattle presentation

$p(\%) \sim A_V^{-\alpha}$

(Note: $A_V \sim I$ for optically thin)

- ❑ $\alpha = 0$: perfect alignment
- ❑ $\alpha = 1$: no alignment
- ❑ $0 < \alpha < 1$: unperfect alignment

$$\omega_{\rm RAT}(a_{\rm align}) = 3\omega_{\rm th}(a_{\rm align})$$

(Hoang & Lazarian 2016)

- ❑ small $a_{\rm align}$: “perfect” alignment
- ❑ large $a_{\rm align}$: “unperfect” alignment
- ❑ $a_{\rm align} > a_{\rm max}$: “no” alignment

Note: max(f(a))<1 for a mixture model of silicate + carbon grains (Draine & Fraisse 2009; Guillet et al. 2018)

3.1 Theoretical calculations (Hoang, Tram et al., submitted to ApJ)

MC without an embedded source: Starless core-like

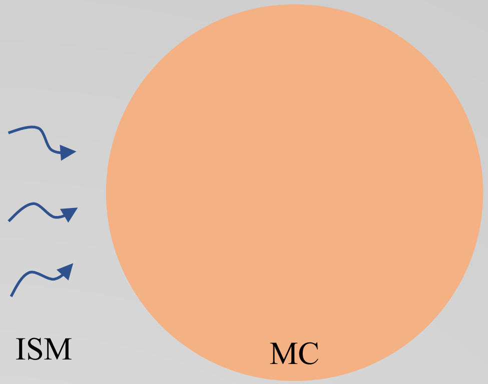

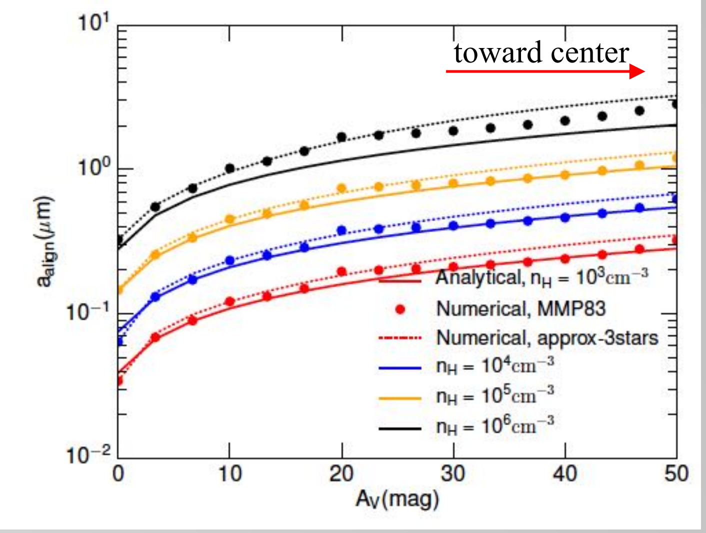

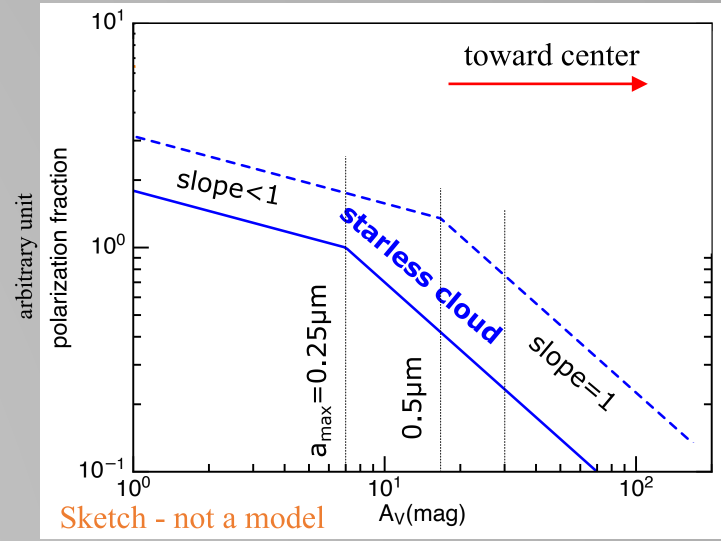

- Analytical results are in excellent agreement with numerical results.
- The alignment size increases gradually with A_V and n_H.
  - ❑ $n_H = 10^4$ cm^{-3}, standard grains ($a < 0.3$ μm) can be aligned upto A_V~10
  - ❑ $n_H > 10^5$ cm^{-3}, only large grains of $a > 0.5$ μm can be aligned at $A_V > 10$

- The degree of dust polarization by dichroic extinction is expected to decrease with increasing A_V
- Grain completely loss alignment: $a_{align} > a_{max}$

See Hoang, Tram et al. 2020 for the detailed calculations

3.1 Theoretical calculations (Hoang, Tram et al., submitted to ApJ)

MC with an embedded source: protostar-like

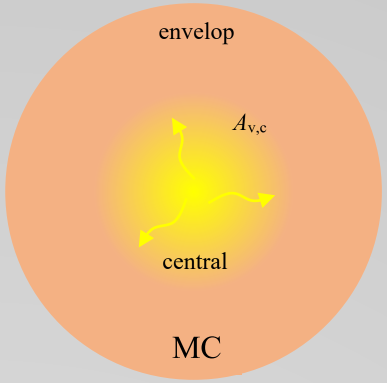

$$n_H(r) = \begin{cases} n_{in} \text{ for } r \le r_{in}, \\ n_{in}\left(\frac{r}{r_{in}}\right)^{-p} \text{ for } r > r_{in}, \end{cases}$$

$$T_{gas} = T_{in}\left(\frac{r}{r_{in}}\right)^{-q}(1 + c_1 A_{V,*}^{c2})^{-q/2},$$

Low-mass protostar
(Visser et al. 2012)

- $n_{in} = 10^8$ cm^{-3}
- $r_{in} = 30$ AU

High-mass protostar
(Bisschop et al. 2007)

- $n_{in} = 10^7$ cm^{-3}
- $r_{in} = 500$ AU

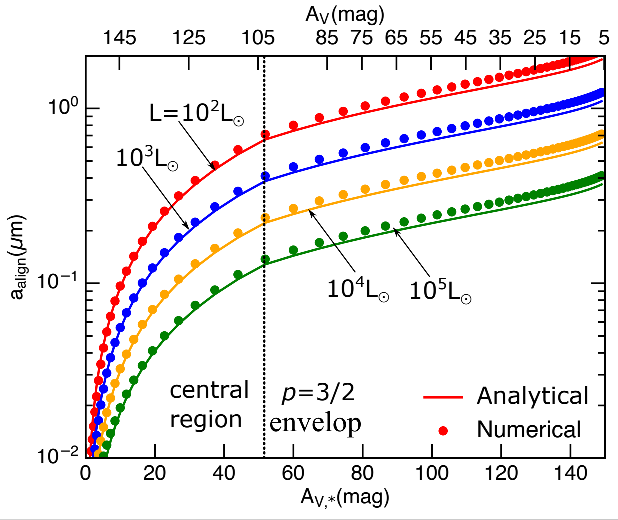

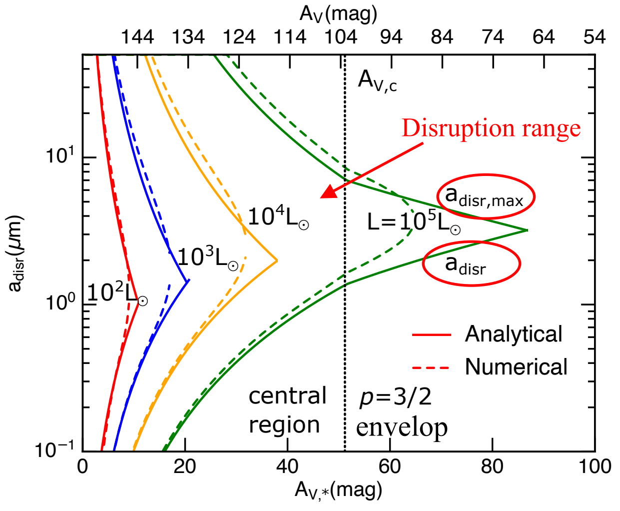

- Analytical results (solid lines) are in good agreement with numerical results (filled circles)
- Alignment size is lower for more luminous sources.
- In the envelope ($A_{V,*} > A_{V,c}$):
  - ❑ the alignment size decreases gradually with decreasing $A_{V,*}$ (increasing A_V)
  - ❑ only large grains can be aligned because of the rapid increase in the gas density as $\sim r^{-p}$
- In the central region ($A_{V,*} < A_{V,c}$): n_H=const, the alignment size decreases rapidly with $A_{V,*}$ due to increase of the radiation intensity.
  - → if the grain size distribution is constant, the polarization of thermal dust emission would increase toward the central protostar producing a slope = 0
  - → we should not see the polarization hole!

- Grains are rotationally disrupted by RATs in the central region.
- The removal of the largest grains by RATD is predicted to reduce p(%) at long wavelength (Lee et al. 2020; Tram, Hoang et al. 2020).

→ p(%)should decrease toward the protostar, and one expects the slope ~0−1

→ produce polarization hole

3.1 Theoretical calculations (Hoang, Tram et al., submitted to ApJ)

MC with an embedded source: protostar-like

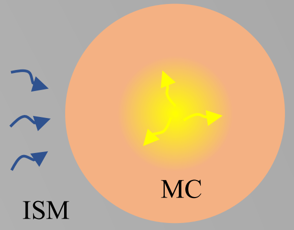

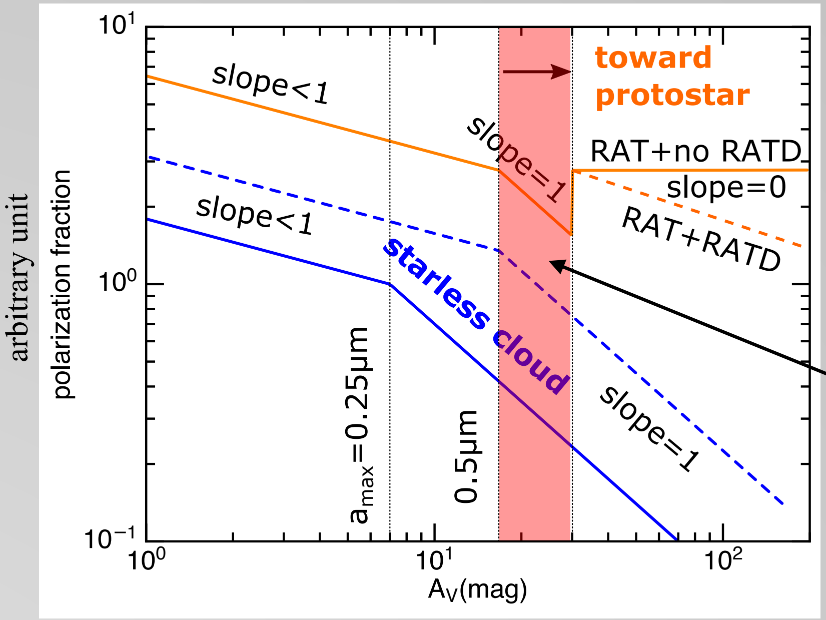

Grain alignment is completely lost

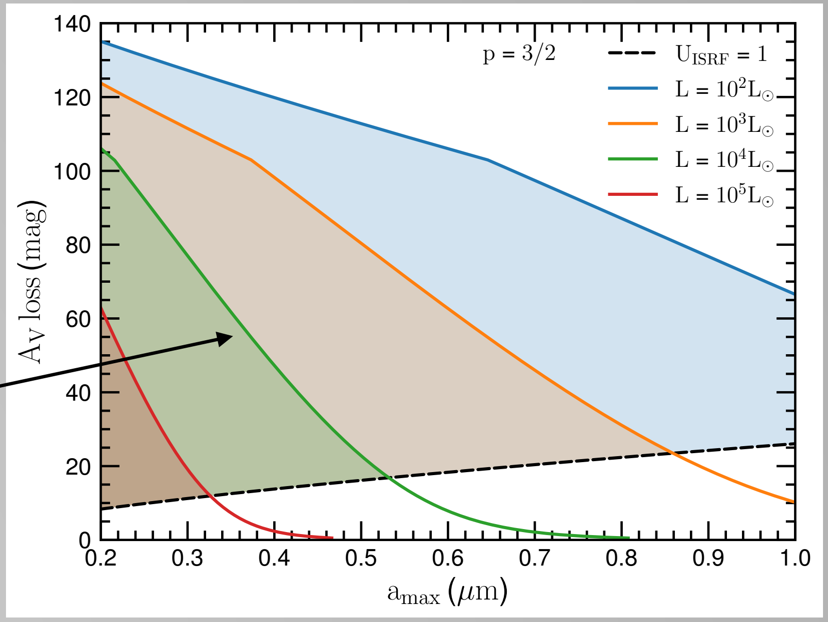

(1) The degree of dust polarization by dichroic extinction is expected to decrease with increasing AV

→(2) Grain completely loss alignment

→(3) Radiation from the source make $p(\%)$ increase

→(4) Disruption effect causes the slope <0

- Loss-alignment zone: shaded regions
- $A_{V,loss}$ depends on the a_{max} and radiation field (internal + external)

3.2 Possible SOFIA/HAWC+ applications

❖ Bok globule B335 (Zielinski, Wolf and Brunngräber 2020)

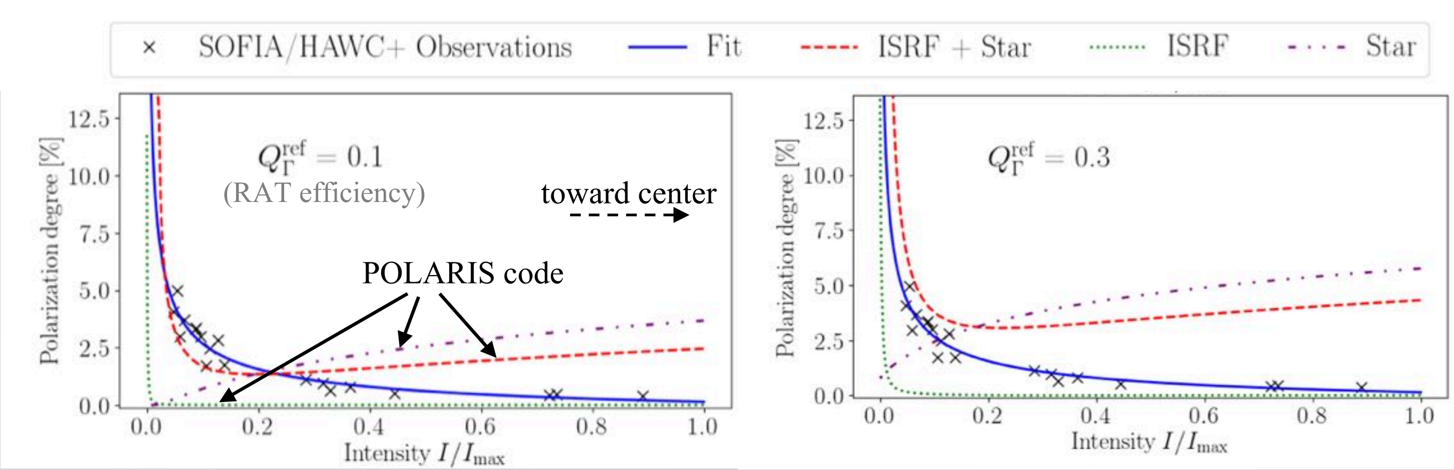

- ISRF alone cannot explain the drop in the $p(\%)$
- Central stellar radiation causes an increase in $p(\%)$ towards the center → contradicting the polarization holes
- ISRF + star leads to a similar slope
- Stronger RAT efficiency → higher $p(\%)$

→ POLARIS model could explain the outer region but cannot explain the decrease in $p(\%)$ towards the center

❖ Serpens South observations (Pillai et al. 2020 Nature Astronomy)

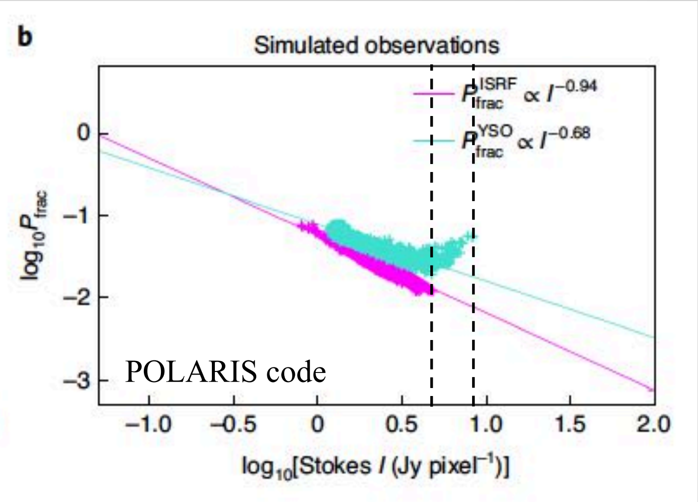

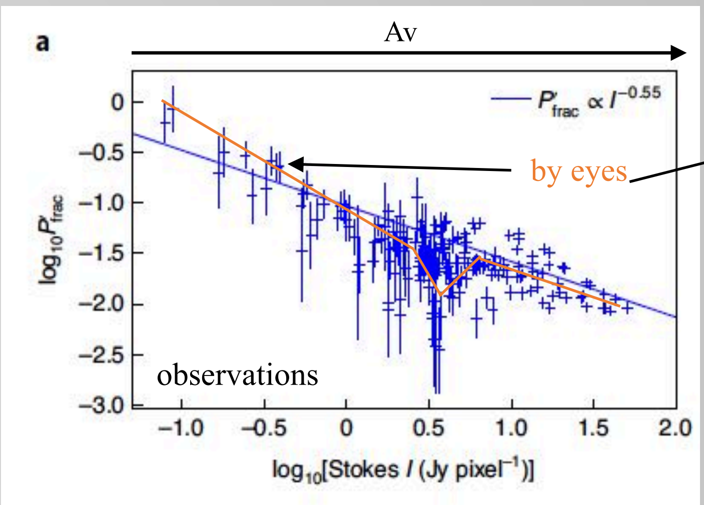

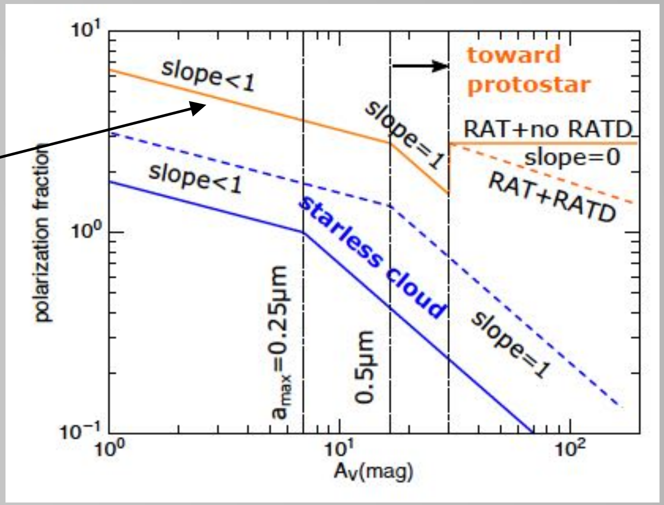

Couldn't change any conclusions in Pillai et al. 2020
It is likely a perfect observational data to test our theory

4. Conclusion

- Large grains exposed to a strong radiation field can be disrupted into smaller species via the RATD mechanism
- RATD mechanism constrains the upper limit for the grain size distribution
- RATD efficiency depends on (n_{H}, T_{d}, U, $S_{\max}$)
- In molecular cloud hosted by a strong radiation source (i.e., a massive star or a cluster of it)
  - joint effect of RAT + RATD reproduces successful the observational $p(\%)$ - T_{d} trend
  - suggests a composite grain structure
  - the power-index of size distribution steeper than the standard MRN distribution (i.e., -3.5)
  - need to be tested in various astrophysical environments/conditions
- RATD could not tell us which sizes are produced via the disruption
  - multiple polarimetric data would help
  - coupling among facilities at different wavelength (SOFIA, JCMT, BLASTPol, APEX) is very important
- Grain alignment and disruption by RAT can explain the polarization hole effect
  - $p(\%)$-A_{V} trend is being developed and implemented to DUSTPOL code
  - need to be tested observationally
- Input parameters are the local parameters
  - prescription will be easy to incorporate into more elaborate models (e.g., POLARIS)
- B-field is assumed to be uniform
  - its variation along l.o.s is being considered in the future work
- RATD can be responsible for other long-standing questions in Astrophysics (see Hoang 2020 for review)

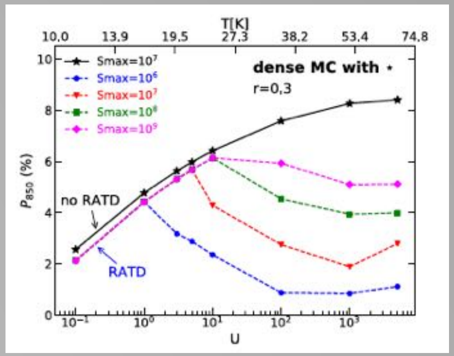

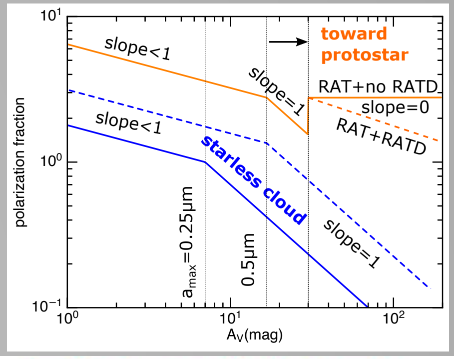

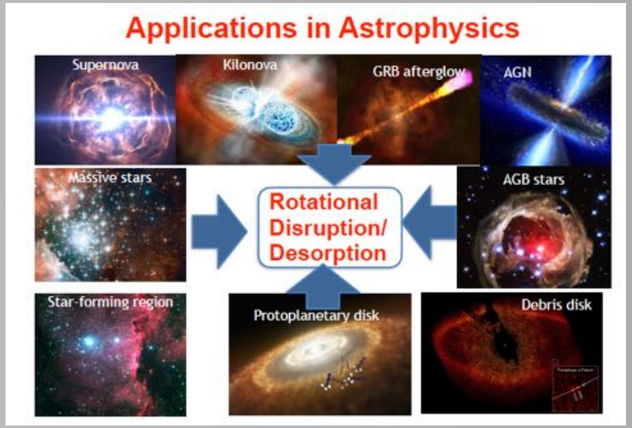

Hoang (2020)

Thank you very much for your time – Xin cảm ơn!